# Energy Harvesting Dynamic Vibration Absorbers

**Shaikh Faruque Ali**
Assistant Professor
Department of Applied Mechanics
Indian Institute of Technology Madras
Chennai 600 036, India
e-mail: sfali@iitm.ac.in

**Sondipon Adhikari**[1]
Professor
Member of ASME
Chair of Aerospace Engineering
College of Engineering
Swansea University Singleton Park,
Swansea SA2 8PP, United Kingdom
e-mail: S.Adhikari@swansea.ac.uk

*Energy harvesting is a promise to harvest unwanted vibrations from a host structure. Similarly, a dynamic vibration absorber is proved to be a very simple and effective vibration suppression device, with many practical implementations in civil and mechanical engineering. This paper analyzes the prospect of using a vibration absorber for possible energy harvesting. To achieve this goal, a vibration absorber is supplemented with a piezoelectric stack for both vibration confinement and energy harvesting. It is assumed that the original structure is sensitive to vibrations and that the absorber is the element where the vibration energy is confined, which in turn is harvested by means of a piezoelectric stack. The primary goal is to control the vibration of the host structure and the secondary goal is to harvest energy out of the dynamic vibration absorber at the same time. Approximate fixed-point theory is used to find a closed form expression for optimal frequency ratio of the vibration absorber. The changes in the optimal parameters of the vibration absorber due to the addition of the energy harvesting electrical circuit are derived. It is shown that with a proper choice of harvester parameters a broadband energy harvesting can be obtained combined with vibration reduction in the primary structure.* [DOI: 10.1115/1.4007967]

## 1 Introduction

The last decade has witnessed many developments in the area of smart structures. Sensors and actuators coupled with a controller that are able to measure and control the dynamic response of structures are designed and deployed for structural health monitoring purposes [1]. The design of control systems has been switched from passive to active, and then to semiactive and hybrid semiactive systems to design efficient and less power demanding systems. One problem that engineers still face is to deploy, maintain, and to power up the sensor and actuator nodes especially in locations that are far reaching and inaccessible. Self-powered or energy autonomous sensors that scavenge energy from the vibration of the host structure seem to be a better alternative to the battery powered sensor nodes.

Many studies are reported in the literature about self-powered or energy autonomous devices, also known as energy harvesting devices, for sensor nodes [2–6]. Most energy harvesting techniques investigated and implemented for structural health monitoring are based on solar energy, thermal gradients, and/or vibration energy. Various concepts of vibration energy harvesting have been proposed [2–5,7–10]. The two main vibration based energy harvesting technologies are electromagnetic and piezoelectric. The electromagnetic harvester generates power from the motion of a coil due to host vibration in a magnetic field [11–13]. Piezoelectric energy harvesters generate power from the strain in piezoelectric materials in response to external mechanical vibrations [14–16]. The advantages of piezoelectric devices include small size, fewer moving parts, and a simpler design. A significant number of studies developed accurate models and discussed in great detail the fundamentals of piezoelectric materials and their usage to harvest energy. These studies include the works of Sodano et al. [17], Shahruz [3], Stephen [18], Ng and Liao [19], Cornwell et al. [20], Lefeuvre et al. [8], Beeby et al. [21], Williams and Yates [11], and Anton and Sodano [5].

Studies reported above focus on the power scavenging efficiency of harvesters. From the application point of view, the main focus has been at structural health monitoring or sensor design of these devices. Research on energy harvesting devices that can be augmented with vibration control are less reported [22–25]. Most notably because when we reduce the vibration of the structure we reduce the power that can be scavenged from it. One needs to find a tradeoff between the vibration reduction and the power harvested. A suitable choice would be a dynamic vibration absorber (DVA), also known as tuned mass dampers (TMDs). This device is used to shift vibrations from the primary structure to the secondary structure (a DVA). The secondary structure then vibrates and releases the energy input to the primary structure. For further details about dynamic vibration absorbers, see for example the book by Den Hartog [26].

Since the vibration energy is effectively localized to a DVA, energy can be scavenged from the DVA instead of the primary structure. This way the "energy harvesting DVA" can be used to simultaneously control and harvest vibration energy of a host structure. Currently DVA is used for passive vibration control in engineering structures such as tall buildings and large flexible bridges due to earthquake or wind excitations. An energy harvesting DVA will give the added benefit of harvesting that energy. Energy scavenged in this way can be used to power wireless sensors or other low-power devices. For example, in the event of a power failure during an earthquake, wireless sensors can be powered by harvested vibration energy. Following these discussions, the current study is concerned with the confinement and harvesting of vibrations in structures by adding a vibration absorber and a piezoelectric element. The proposed design aims at transferring the vibration energy from the structure to the absorbers and confining it into stack piezoelectric elements.

## 2 Energy Harvesting Dynamic Vibration Absorber

A schematic diagram of the proposed energy harvesting dynamic vibration harvester (EHDVA) is shown in Fig. 1. This is a coupled two degree of freedom electromechanical system with in general nonproportional damping [27,28]. The primary mass ($m_0$) whose vibrations has to be reduced is augmented with the DVA (mass $m_h$). The DVA consists of a spring, a damping, and a piezoelectric element to harvest energy. The piezoelectric element is attached to the electric circuit as shown in Fig. 1.

**2.1 Dynamic Vibration Absorber and the Fixed-Point Theory.** A dynamic vibration absorber is a widely used passive vibration control device. When a primary system is subjected to a

[1]Corresponding author.

Contributed by the Energy Division of ASME for publication in the JOURNAL OF APPLIED MECHANICS. Manuscript received August 3, 2011; final manuscript received October 18, 2012; accepted manuscript posted October 30, 2012; published online May 16, 2013. Assoc. Editor: Alexander F. Vakakis.

  

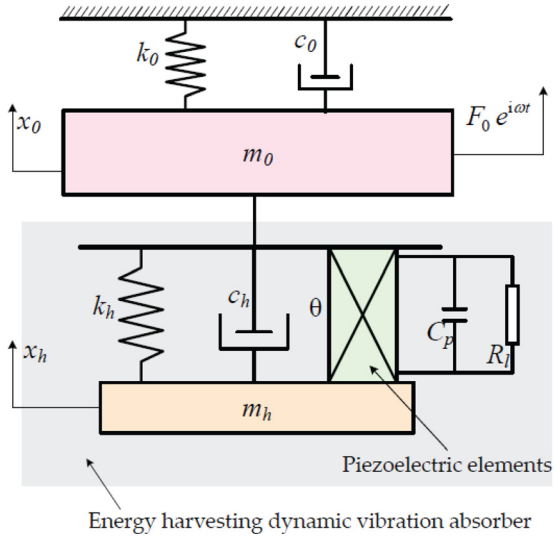


**Fig. 1 Schematic diagram of the energy harvesting dynamic vibration absorber attached to a single degree of freedom vibrating system**

harmonic excitation at a constant frequency, its steady-state response can be suppressed by attaching a secondary mass-spring system or DVA. However, a DVA consisting of only a mass and a spring has a narrow operation region and its performance deteriorates significantly when the exciting frequency varies. The performance robustness can be improved by using a damped DVA. The key design parameters of a damped DVA are its tuning parameter (also known as the frequency ratio) and the damping ratio.

The first mathematical theory on the damped DVA was presented by Ormondroyd and Den Hartog [29]. Den Hartog [26] first found the optimum solution of a damped DVA that is attached to a damping-free primary system. His study utilized the novel idea of "fixed-point" frequencies, that is, the frequencies at which the response amplitudes of the primary mass are independent of the absorber damping. The theory states the existence of two fixed points $P$ and $Q$ in the frequency response curves of the displacement of the primary structure. The points $P$ and $Q$ are independent of the damping in the absorber as shown in Fig. 2(*a*). This reduces the optimization parameters only to the frequency ratio. Based on the fixed-point theory, Den Hartog found the optimum tuning parameter and defined the optimality for the optimum absorber damping.

As shown in Fig. 2(*b*), when a primary system is damped, the usefulness of the fixed-points feature is no longer strictly valid. Thus, obtaining an exact closed-form solution for the optimum tuning parameter or optimum damping ratio becomes very difficult. A number of studies have focused on the approximate and numerical solutions. These include numerical optimization schemes proposed by Randall et al. [30,31], nonlinear programming techniques by Liu and Coppola [32], frequency locus method by Thompson [33], and min-max Chebyshev's criterion by Pennestri [34] to name a few. Numerical studies based on minimax optimization are reported in [24,35]. In spite of being exact, these analyses are usually problem specific and may not give physical insights to the phenomenon for the general case.

Ghosh and Basu [36] identified that for small damping in the primary system, although there exist no points like $P$ and $Q$ in a strict sense, the fixed-point theory can be applied. Ghosh and Basu [36] derived an approximate analytical solution for the optimum tuning parameter based on the assumption that the fixed-points theory also approximately holds when a damped DVA is attached to a lightly or moderately damped primary system (see Fig. 2(*b*)). Motivated by this, we develop a fixed-point theory for the coupled electromechanical system. We aim to provide an analytical derivation of the power harvested by an energy harvesting DVA. The optimal DVA parameters which reduce the primary structure vibrations as well as harvest maximum power will be given.

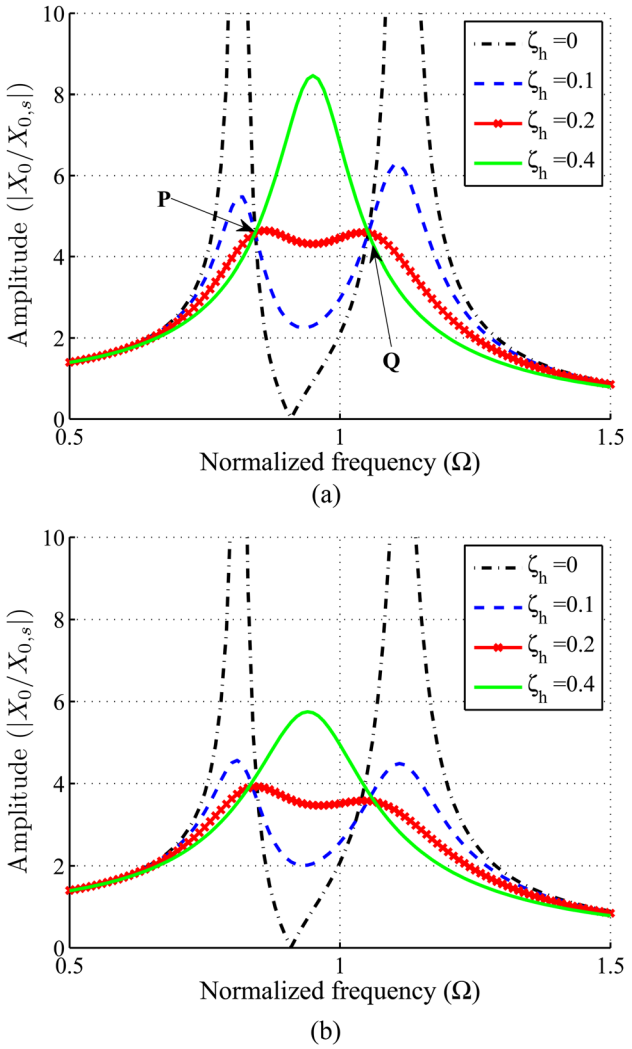


**Fig. 2 Frequency response of the primary mass in a classical dynamic vibration absorber for mass ratio $\mu = 0.1$ at optimal frequency ratio $\beta = \sqrt{1/(1+\mu)}$. (*a*) Without any damping in primary structure and (*b*) with primary structure damping. $\zeta_h$ in the figures represents the damping ratio in the absorber.**

**2.2 Dynamic Vibration Absorber With Energy Harvesting.** The primary structure is assumed to be a single degree of freedom system as shown in Fig. 1. The mass, stiffness, and the damping of the primary structure are represented by $m_0$, $k_0$, and $c_0$, respectively, whereas the energy harvesting DVA has an equivalent mass, equivalent stiffness, and damping as $m_h$, $k_h$, and $c_h$, respectively. The electrical capacitance and resistance are denoted by $C_p$ and $R_l$, respectively. The variable $\theta$ is the coupling between the electrical and mechanical parts of the harvester. The dynamics of the primary mass ($m_0$), the absorber mass ($m_h$), and voltage flow can be expressed by three coupled ordinary differential equations as

$$m_0\ddot{x}_0 + c_0\dot{x}_0 + k_0x_0 - k_h(x_h - x_0) - c_h(\dot{x}_h - \dot{x}_0) = F_0e^{i\omega t} \quad (1)$$

$$m_h\ddot{x}_h + c_h(\dot{x}_h - \dot{x}_0) + k_h(x_h - x_0) - \theta v = 0 \quad (2)$$

$$C_p\dot{v} + \frac{v}{R_l} + \theta\dot{x}_h = 0 \quad (3)$$

where $x_0$ and $x_h$ are the displacement of the primary mass and absorber mass, respectively. The voltage across the load resistor is denoted by $v$. The electromechanical coupling and the mechanical force are modeled as proportional to the voltage across the piezoceramic in Eq. (2). Equation (3) is obtained from the electrical circuit, where the voltage across the load resistance arises from the mechanical strain through the electromechanical coupling, and the capacitance of the piezoceramic $C_p$. The primary structure is assumed to be driven by a harmonic excitation with amplitude $F_0$.

The steady state solution of Eqs. (1)–(3) can be written as

$$x_0 = X_0 e^{i\omega t}, \quad x_h = X_h e^{i\omega t}, \quad \text{and} \quad v = V e^{i\omega t} \tag{4}$$

Substituting Eq. (4) into Eqs. (1)–(3) and then normalizing with respect to the resonance frequency of the primary mass $\omega_0 = \sqrt{k_0/m_0}$, we get

$$\left[-\Omega^2 + 2(\zeta_0 + \zeta_h\mu\beta)i\Omega + (1+\mu\beta^2)\right]X_0 - \mu(2\zeta_h\beta i\Omega + \beta^2)X_h = F_0/k_0 \tag{5}$$

$$-(2\zeta_h\beta i\Omega + \beta^2)X_0 + \left[-\Omega^2 + 2\zeta_h\beta i\Omega + \beta^2\right]X_h - \frac{\theta}{k_h}\beta^2 V = 0 \tag{6}$$

$$\frac{\theta\alpha}{C_p} i\Omega X_h + (\beta + \alpha i\Omega)V = 0 \tag{7}$$

Here $\mu = m_h/m_0$ is the ratio of the absorber mass to the primary mass, known as mass ratio, $\beta = \omega_h/\omega_0$ is the ratio of the decoupled absorber frequency to the natural frequency of the primary structure, known as frequency ratio, $\Omega = \omega/\omega_0$ is the nondimensional frequency of excitation, and $\alpha = \omega_n C_p R_l$ is the dimensionless time constant. The coefficient of damping in the primary structure is given by $\zeta_0 = c_0/(2m_0\omega_0)$, whereas $\zeta_h = c_h/(2m_h\omega_h)$ is the damping coefficient of the absorber.

Solving Eqs. (5)–(7) for the displacement amplitudes $X_0$ and $X_h$, and for the voltage amplitude $V$, we get

$$\left|\frac{X_0}{F_0/k_0}\right| = \frac{\left[a_{0_0} + a_{0_2}(i\Omega)^2\right]^2 + \left[a_{0_1}(i\Omega) + a_{0_3}(i\Omega)^3\right]^2}{|\Delta|^2} \tag{8}$$

$$\left|\frac{X_h}{F_0/k_0}\right| = -\frac{\left[a_{h_0} + a_{h_2}(i\Omega)^2\right]^2 + [a_{h_1}(i\Omega)]^2}{|\Delta|^2} \tag{9}$$

$$\left|\frac{V}{F_0/k_0}\right| = \frac{\left[a_{v_0} + a_{v_2}(i\Omega)^2\right]^2 + [a_{v_1}(i\Omega)]^2}{|\Delta|^2} \tag{10}$$

Note that Eqs. (8)–(10) are normalized with respect to the static displacement of the primary structure ($F_0/k_0$) to make the expressions on the right-hand side independent of the excitation amplitude. The denominator is given as

$$\Delta = b_0 + b_1(i\Omega) + b_2(i\Omega)^2 + b_3(i\Omega)^3 + b_4(i\Omega)^4 + b_5(i\Omega)^5 \tag{11}$$

The coefficients appearing in Eqs. (8)–(11) are given by

$$\begin{aligned}
&a_{0_0} = \beta^3, \quad a_{0_1} = (\alpha + 2\zeta_h + \alpha\kappa^2)\beta^2, \quad a_{0_2} = (2\zeta_h\alpha + 1)\beta, \quad a_{0_3} = \alpha,\\
&a_{h_0} = \beta^3, \quad a_{h_1} = (\alpha + 2\zeta_h)\beta^2, \quad a_{h_2} = (2\zeta_h\alpha\beta),\\
&a_{v_0} = 0, \quad a_{v_1} = -\frac{\theta\alpha}{C_p}\beta^2, \quad a_{v_2} = -\frac{2\zeta_h\theta\alpha}{C_p}\beta
\end{aligned}$$

and

$$\begin{aligned}
b_0 &= \beta^3\\
b_1 &= \beta^4\alpha\kappa^2\mu + 2\beta^3\zeta_0 + (\alpha + 2\zeta_h + \alpha\kappa^2)\beta^2\\
b_2 &= (2\alpha\kappa^2\zeta_h\mu + 1 + \mu)\beta^3 + (2\alpha\kappa^2\zeta_0 + 2\alpha\zeta_0 + 4\zeta_h\zeta_0)\beta^2 + (2\zeta_h\alpha + 1)\beta\\
b_3 &= (\alpha + \alpha\kappa^2 + \alpha\mu + 2\zeta_h\mu + 2\zeta_h)\beta^2 + (2\zeta_0 + 4\alpha\zeta_h\zeta_0)\beta + \alpha\\
b_4 &= [(2\zeta_h\mu + 2\zeta_h)\alpha + 1]\beta + 2\alpha\zeta_0\\
b_5 &= \alpha
\end{aligned}$$

where $\kappa^2 = \theta^2/(k_h C_p)$ is the nondimensional time constant for the electrical part.

The objective is to reduce the vibration of the primary mass (minimize $X_0$ / ($F_0$ / $k_0$)) and simultaneously scavenge as much energy as possible (maximize $V$ / ($F_0$ / $k_0$)) from it using the piezoelectric harvester. Straightforward optimization of a cost function containing both terms will result in solving a tenth order polynomial in $\Omega$. A brute-force numerical optimization approach is certainly possible, but may not give desirable physical insights. An alternative route would be to follow a slightly different approach as pioneered by Den Hartog [26,29], Ghosh and Basu [36], and Liu and Coppola [32]. The additional complexity in the analysis reported in this paper compared to the results from the above references is due to the addition of Eq. (3) to the DVA system.

## 3 Development of the Fixed-Point Theory

For the development of the fixed-point theory we assume that the primary system parameters like $m_0$, $k_0$, and $c_0$ are known. We need to find the optimal mechanical parameters for the secondary system that are $k_h$ and $\zeta_h$ and the electrical parameters like $\alpha$ and $\kappa$ when the mass ratio $\mu$ is given. Theoretically, even when we put $\zeta_0 = 0$ in Eq. (8), the fixed-point theory does not hold due to the coupling with Eq. (3). But for all practical purposes and for small values of $\kappa$, although there exist no points like $P$ and $Q$, the fixed-point theory can be applied approximately as has been shown by Ghosh and Basu [36].

The frequency response curves of the primary structure displacement with EHDVA for various combinations of $\mu$, $\kappa^2$, and $\alpha$ are shown in Figs. 3(*a*)–3(*d*). The range of nondimensional coefficient $\kappa^2$ is taken up to 0.4. Note that this value is quite high for energy harvesting systems as the optimal value usually lies between 0.1 and 0.2 [15,16]. The nature of curves for different $\kappa^2$ values and $\alpha$ values are shown in Fig. 3. It can be observed from these figures that for low mass ratio, for different values of nondimensional coupling coefficient and nondimensional time constants, the frequency curves roughly pass through two fixed points similar to the classical case considered by Den Hartog [26,29]. We therefore use the fixed-point theory to simplify further analysis. We also assume that the damping in the primary mass is negligible as most structures have very little inherent damping. Substituting $\zeta_0 = 0$, from Eq. (8) one obtains the response of the primary mass as

$$\left|\frac{X_0}{F_0/k_0}\right| = \frac{a_{0_\zeta} + a_{1_\zeta}\zeta_h + a_{2_\zeta}\zeta_h^2}{b_{0_\zeta} + b_{1_\zeta}\zeta_h + b_{2_\zeta}\zeta_h^2} \tag{12}$$

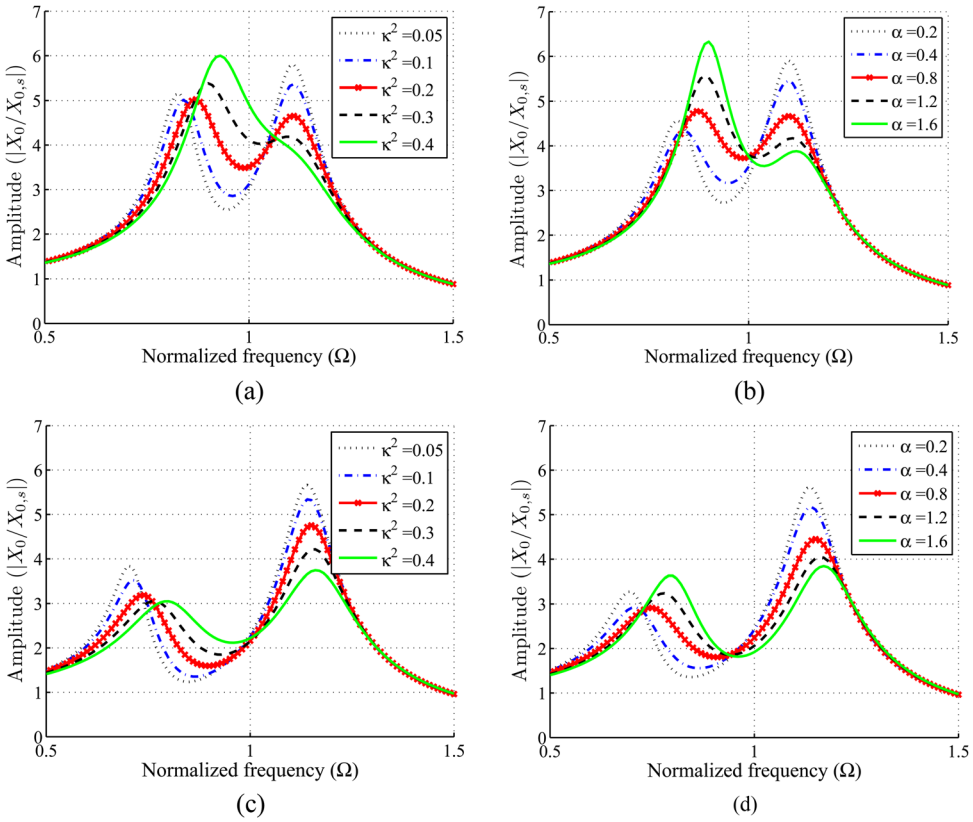


**Fig. 3 Frequency response of the displacement of the primary mass with the energy harvesting vibration absorber for different mass ratio and electrical coefficients and with optimal frequency ratio (Eq. (24)), absorber damping $\zeta_h = 0.01$, and undamped primary structure**

where

$$a_{0_\zeta} = \alpha^2\Omega^6 + \left(-2\beta^2\alpha^2 + \beta^2 - 2\beta^2\alpha^2\kappa^2\right)\Omega^4 + \left(-2\beta^4 + \beta^4\alpha^2 + 2\beta^4\alpha^2\kappa^2 + \beta^4\alpha^2\kappa^4\right)\Omega^2 + \beta^6$$

$$a_{1_\zeta} = 4\beta^4\alpha\kappa^2\Omega^2, a_{2_\zeta} = 4\left(\Omega^2\alpha^2 + \beta^2\right)\beta^2\Omega^2$$

$$b_{0_\zeta} = \alpha^2\Omega^{10} + \left(-2\beta^2\alpha^2 - 2\beta^2\alpha^2\mu - 2\alpha^2 - 2\beta^2\alpha^2\kappa^2 + \beta^2\right)\Omega^8 + \begin{pmatrix} -2\beta^4\mu + 4\beta^4\alpha^2\kappa^2\mu + 2\beta^4\alpha^2\kappa^2 - 2\beta^4 - 2\beta^2 + \alpha^2 + 4\beta^2\alpha^2\kappa^2 \\ +\beta^4\alpha^2 + \beta^4\alpha^2\kappa^4 + \beta^4\alpha^2\mu^2 + 4\beta^2\alpha^2 + 2\beta^2\alpha^2\mu + 2\beta^4\alpha^2\mu \end{pmatrix}\Omega^6$$
$$+ \begin{pmatrix} -4\beta^4\alpha^2\kappa^2\mu - 2\beta^4\alpha^2\kappa^4 + \beta^6 + 4\beta^4 + \beta^2 - 2\beta^2\alpha^2\kappa^2 - 2\beta^6\alpha^2\kappa^2\mu^2 \\ +\beta^6\mu^2 + 2\beta^6\mu - 2\beta^2\alpha^2 - 2\beta^4\alpha^2 - 2\beta^4\alpha^2\mu + 2\beta^4\mu - 4\beta^4\alpha^2\kappa^2 \\ -2\beta^6\alpha^2\kappa^4\mu - 2\beta^6\alpha^2\kappa^2\mu \end{pmatrix}\Omega^4$$
$$+ \begin{pmatrix} \beta^4\alpha^2 + \beta^8\alpha^2\kappa^4\mu^2 - 2\beta^4 + 2\beta^4\alpha^2\kappa^2 \\ +2\beta^6\alpha^2\kappa^2\mu + 2\beta^6\alpha^2\kappa^4\mu - 2\beta^6 - 2\beta^6\mu + \beta^4\alpha^2\kappa^4 \end{pmatrix}\Omega^2 + \beta^6$$

$$b_{1_\zeta} = 4\beta^4\Omega^2\alpha\kappa^2 - 8\beta^4\alpha\kappa^2\Omega^4 + 4\beta^4\alpha\kappa^2\Omega^6$$

$$b_{2_\zeta} = \left(4\beta^2\alpha^2 + 8\beta^2\alpha^2\mu + 4\beta^2\alpha^2\mu^2\right)\Omega^8 + \left(-8\beta^4\alpha^2\kappa^2\mu - 8\beta^4\alpha^2\kappa^2\mu^2 - 8\beta^2\alpha^2 + 4\beta^4 - 8\beta^2\alpha^2\mu + 4\beta^4\mu^2 + 8\beta^4\mu\right)\Omega^6$$
$$\times \left(-8\beta^4 - 8\beta^4\mu + 4\beta^2\alpha^2 + 4\beta^6\alpha^2\kappa^4\mu^2 + 8\beta^4\alpha^2\kappa^2\mu\right)\Omega^4 + 4\beta^4\Omega^2$$

In classical DVA the fixed points $P$ and $Q$ are independent of DVA damping. Therefore any damping values can be considered for analysis. Let us substitute $\zeta_h = 0$ and $\zeta_h = \infty$ in Eq. (12). We have

$$\lim_{\zeta_h \to 0}\left|\frac{X_0}{F_0/k_0}\right| = \frac{a_{0_\zeta}}{b_{0_\zeta}} \tag{13}$$

and

$$\lim_{\zeta_h \to \infty} \left| \frac{X_0}{F_0/k_0} \right| = \frac{a_{2_\zeta}}{b_{2_\zeta}} \tag{14}$$

Since the fixed points are independent of damping, equating Eqs. (13) and (14) and then rewriting them in terms of $\kappa$, we get

$$a_{0_\kappa} + a_{2_\kappa}\kappa^2 + a_{4_\kappa}\kappa^4 = 0 \tag{15}$$

where

$$\begin{aligned}
a_{0_\kappa} &= \Omega^2\left(\beta^2+\alpha^2\Omega^2\right)^2\left\{(2+\mu)\Omega^4 - \left[2(1+\mu)\beta^2+1\right]\Omega^2+2\beta^2\right\}\\
a_{2_\kappa} &= -2\beta^2\alpha^2\Omega^2\left(\beta^2+\alpha^2\Omega\right)\left\{\begin{matrix}(2\mu+3)\Omega^4-\left[(2+3\mu)\beta^2+3\right]\Omega^2\\ +2\beta^2\end{matrix}\right\}\\
a_{4_\kappa} &= 2\beta^4\alpha^2\left\{\begin{matrix}3(1+\mu)\alpha^2\Omega^6+\left\{\left[(1+\mu)-(1+3\mu)\alpha^2\right]\beta^2-3\alpha^2\right\}\Omega^4\\ +\left[(1-\mu)\beta^4+(\alpha^2-1)\beta^2\right]\Omega^2+\beta^4\end{matrix}\right\}
\end{aligned} \tag{16}$$

Equation (15) with coefficients given by Eqs. (16) represents a third-order polynomial in $\Omega^2$. A simple analytical solution for $\Omega$ is hard to obtain. We can approximate the above function by assuming $\kappa^2$ to be small. Neglecting the fourth and higher order terms in $\kappa$, Eq. (15) reduces to

$$(2+\mu)\Omega^4 - 2\left[(1+\mu)\beta^2+1\right]\Omega^2 + 2\beta^2 = 0 \tag{17}$$

Equation (17) is obtained for the undamped primary system with only an absorber and no harvester circuit attached to it. Solution of Eq. (17) gives same values for $\Omega_P$ and $\Omega_Q$ as Den Hartog's solution in [26] and the same expression in $\Omega$ is reported in [36].

## 4 Optimal Mechanical Parameters

**4.1 Optimal Tuning Parameter.** Once the fixed-points frequencies are determined, the nest task is to optimize $\beta$. The optimum tuning ratio $\beta$ is the one for which the values of $[X_0/F_0/k_0]_{\Omega=\Omega_P}$ equals $[X_0/F_0/k_0]_{\Omega=\Omega_Q}$ for all possible choices of $\zeta_h$ [26,36]. Substituting $\Omega=\Omega_P$ and $\Omega=\Omega_Q$ separately in Eq. (12) and then equating the resulting expressions, we get

$$\left[\frac{a_{0_\zeta}+a_{1_\zeta}\zeta_h+a_{2_\zeta}\zeta_h^2}{b_{0_\zeta}+b_{1_\zeta}\zeta_h+b_{2_\zeta}\zeta_h^2}\right]_{\Omega=\Omega_P} = \left[\frac{a_{0_\zeta}+a_{1_\zeta}\zeta_h+a_{2_\zeta}\zeta_h^2}{b_{0_\zeta}+b_{1_\zeta}\zeta_h+b_{2_\zeta}\zeta_h^2}\right]_{\Omega=\Omega_Q} \tag{18}$$

When $\zeta_h \to \infty$ in Eq. (18) we obtain

$$\left[\frac{a_{2_\zeta}}{b_{2_\zeta}}\right]_{\Omega=\Omega_P} = \left[\frac{a_{2_\zeta}}{b_{2_\zeta}}\right]_{\Omega=\Omega_Q} \tag{19}$$

Substituting Eq. (20) derived from Eqs. (17) to (19),

$$\begin{aligned}
\Omega_P^2+\Omega_Q^2 &= \frac{2(1+\mu)\beta^2+2}{2+\mu}\\
\Omega_P^2\Omega_Q^2 &= \frac{2\beta^2}{2+\mu}
\end{aligned} \tag{20}$$

we get a polynomial in $\beta$ as

$$a_{0_\beta} + a_{2_\beta}\beta^2 + a_{4_\beta}\beta^4 = 0 \tag{21}$$

The coefficients appearing in this polynomial are given as

$$\begin{aligned}
a_{0_\beta} &= 2\alpha^2\left(\alpha^2+1\right)(\mu+1)\\
a_{2_\beta} &= -2\left[\left(1-\kappa^2\right)\mu^3+3\left(1-\kappa^2\right)\mu^2+\left(3-2\kappa^2\right)\mu+1\right]\alpha^4\\
&\quad -\left[\left(2-\kappa^2\right)\mu^3+2\left(2-\kappa^2\right)\mu^2+2\mu\right]\alpha^2+(1+\mu)(2+\mu)\\
a_{4_\beta} &= -\left\{\begin{matrix}\tfrac{1}{2}(2-\kappa^2)^2\mu^4+2(2-\kappa^2)^2\mu^3\\ +2(3-\kappa^2)(2-\kappa^2)\mu^2+4(2-\kappa^2)\mu+2\end{matrix}\right\}\\
&\quad \alpha^2-(1+\mu)^3(2+\mu)
\end{aligned} \tag{22}$$

One can solve Eq. (21) for various parametric values and can find optimal frequency ratio $\beta$. The general solution is given as

$$\beta^2 = \frac{-a_{2_\beta} \pm \sqrt{a_{2_\beta}^2 - 4a_{4_\beta}a_{0_\beta}}}{2a_{4_\beta}} \tag{23}$$

Analysis of coefficients $a_{0_\beta}$, $a_{2_\beta}$, and $a_{4_\beta}$ in Eq. (22) will reveal that $a_{0_\beta} \geq 0$ and $a_{4_\beta} \leq 0$ for all values of $0 \leq \kappa^2 < 2$, and for all positive values of $\alpha$ and $\mu$. Therefore for a real, positive optimal value of $\beta$ we have

$$\beta^2 = \frac{-a_{2_\beta} - \sqrt{a_{2_\beta}^2 - 4a_{4_\beta}a_{0_\beta}}}{2a_{4_\beta}} \tag{24}$$

Substituting $\alpha=0$ in Eq. (21) we get

$$-(1+\mu)^2\beta^4 + \beta^2 = 0 \tag{25}$$

Equation (25) gives the Den Hartog [26] solution of either $\beta=1/(1+\mu)$ or $\beta=0$. $\beta=1/(1+\mu)$ provides an optimal solution for a simple DVA mounted on an undamped structure, whereas the second solution $\beta=0$ represents the trivial case for a static system. Equation (24) can be viewed as the generalization of the solutions for classical DVA to energy harvesting DVA and one of the key findings in this paper. Solution to Eq. (24) is shown in Fig. 4 for different values of $\kappa^2$ and $\alpha$. Den Hartog's solution can be retrieved when $\alpha=0$ and $\kappa^2=0$. Once the natural frequency of the primary system is known, this curve can provide the details

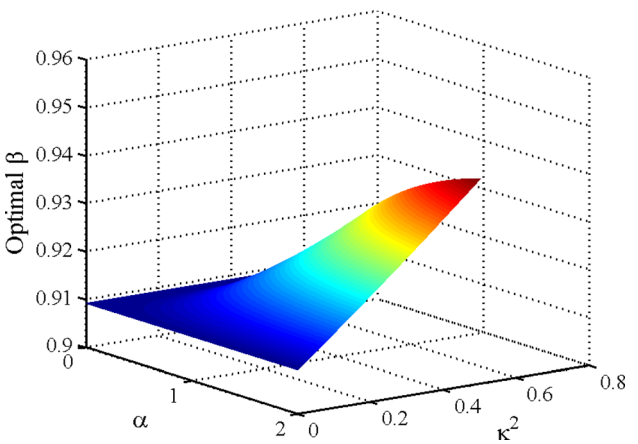


**Fig. 4 Optimal values of ratio of decoupled natural frequencies ($\beta$) for various values of $\alpha$ and $\kappa^2$. Optimal values of the frequency ratio seems to be a linear function of the square of the nondimensional coupling coefficient. This is from the approximation that neglects higher order in $\kappa^2$.**

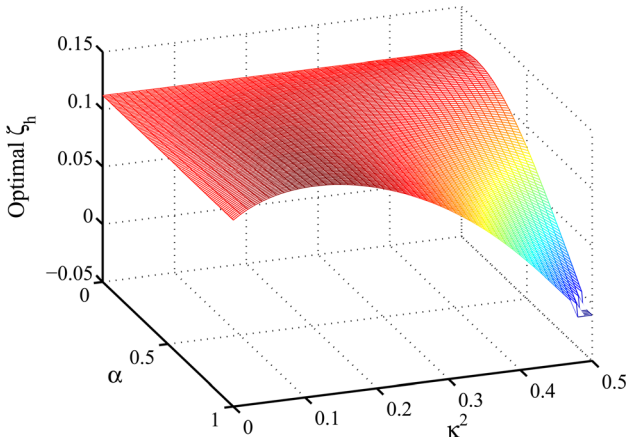


**Fig. 5 Optimal damping of the EHDVA ($\zeta_h$) for various values of $\alpha$ and $\kappa^2$**

for the natural frequency of the DVA for different values of the nondimensional harvester parameters ($\alpha$ and $\kappa^2$).

**4.2 Optimal Damping Factor.** There are two ways to find the optimal damping for the absorber. Den Hartog [26] reported that the optimal $\zeta_h$ is the one for which the amplitude curve passes horizontally through the points $P$ and $Q$. The idea is to take the derivative of the expression in Eq. (12) with respect to $\Omega$. Then substitute the value of $\Omega_P$ from Eq. (17) into the resulting expression and equate it to zero. This analysis provides two different optimal values for DVA damping. One can take an average of the two to get the optimal damping.

Another technique is based on the assumption that at optimal damping the frequency response curve of $X_0/X_{0,s}$ will be parallel to the frequency axis between the fixed points and therefore will have the same amplitude between these points. The idea is to equate the amplitudes at either point $P$ or $Q$ with the amplitude at a frequency which represents a rigid connection between the DVA and the primary structure, i.e., $\omega_\infty = \sqrt{k_0/(m_0 + m_h)}$.

We follow the later method. Figure 5 shows the optimal damping $\zeta_h$ as against the nondimensional time constant $\alpha$ and the nondimensional coupling coefficient $\kappa^2$. An increase in the values of $\alpha$ and $\kappa^2$ decreases the values of optimal $\zeta_h$, i.e., with the addition of the harvesting circuit the overall damping in the DVA is increased. This decreases the high damping requirement for optimal performance. The optimal $\zeta_h$ values sharply decrease to zero. We have pointed out that the fixed-point theory is applicable for small values of $\alpha$ and $\kappa^2$. For higher values of $\alpha$ and $\kappa^2$, the analysis may not provide a real solution to the optimal $\zeta_h$ value.

## 5 Optimal Electrical Parameter and Harvested Power

In this section we consider the response of the primary system and energy harvested from the secondary system. The power harvested from the energy harvesting DVA is given by [15,37]

$$P = \frac{|V|^2}{R_l} = \frac{|V|^2}{\alpha} C_p \omega_h \tag{26}$$

The harvester resistance is assumed to be fixed in Eq. (26) and therefore the power depends only on the square of the voltage. Figure 6 shows the frequency response curves of the primary mass displacement (Figs. 6(*a*) and 6(*b*)) against $\alpha$ and $\kappa^2$. The qualitative nature of the curves are similar. At low values of $\alpha$ there exists two peaks but these two peaks dissolve into one as the value of $\alpha$ increases. This implies that with the increase in the values of the electrical parameters, the system effectively behaves as a single-degree-of-freedom system and the relative motion between the masses decreases. A close observation of Figs. 6(*a*)

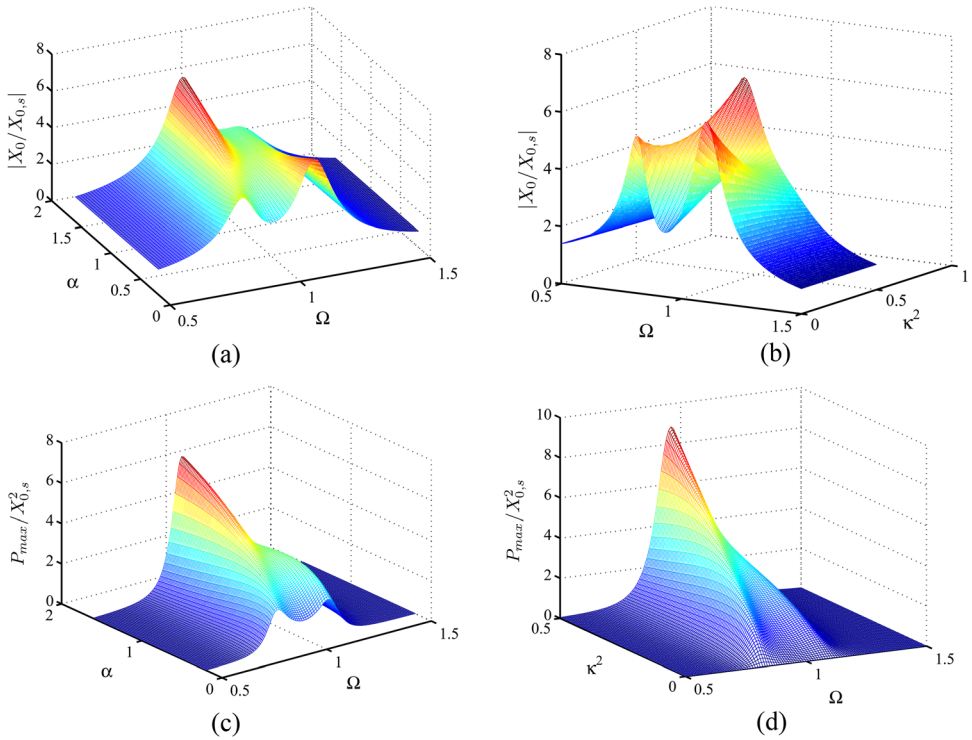


**Fig. 6 Frequency response curves of the primary structure (*a*) and (*b*) normalized displacement and (*c*) and (*d*) normalized power for various values of nondimensional time constant $\alpha$ and nondimensional coupling coefficient $\kappa^2$ for mass ratio $\mu = 0.1$, optimal frequency ratio $\beta$ and harvester damping as $\zeta_h = 0.1$. The responses are normalized with respect to static displacement of the primary structure $F_0 / k_0 = X_{0,s}$.**

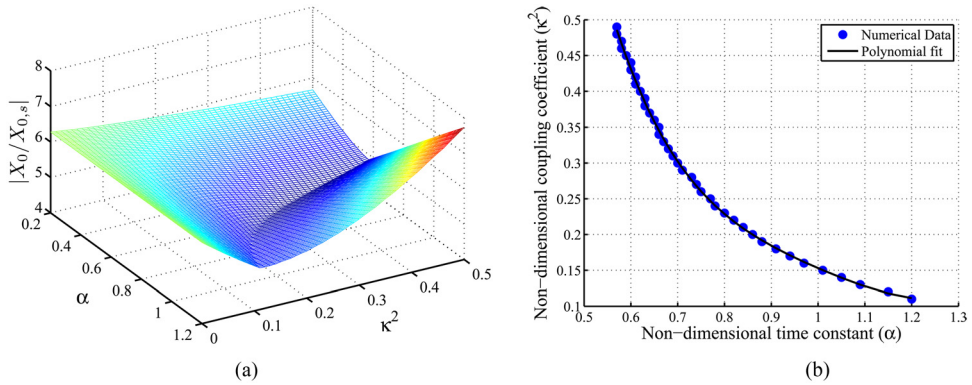


**Fig. 7 (*a*) Peak normalized primary structure displacement for different values of nondimensional time constant ($\alpha$) and nondimensional coupling coefficient with mass ratio $\mu = 0.1$, damping $\zeta_h = 0.1$, and optimal frequency ratio. (*b*) Numerically obtained from (*a*) and polynomial fit of nondimensional electrical parameters ($\alpha$ and $\kappa^2$).**

and 6(*b*) shows that there exist values for $\alpha$ and $\kappa^2$ for which the curve attains a minimum.

Frequency response curves of the harvested power against $\alpha$ and $\kappa^2$ are shown in Figs. 6(*c*) and 6(*d*), respectively. Equation (26) is used to plot the power harvested, where Eq. (10) is used to calculate $|V|^2$. The power plots are normalized with respect to the square of the static displacement of the primary structure ($X_{0,s} = F_0 / k_0$). As discussed before the power curves are bimodal at low $\alpha$ and $\kappa^2$ values. At higher values the power curves are unimodal. This gives us a chance to decide the optimal values of the electrical parameters from the frequency response curves. Since at lower values of the electrical parameters, the energy harvesting DVA has a bimodal frequency response, this could be used for broadband energy harvesting.

Figure 7 shows the maximum of the normalized displacement response of the primary structure for various values of $\alpha$ and $\kappa^2$. It is evident from the figure that there exist different values for $\alpha$ and $\kappa^2$ for which the peak displacement amplitude of the primary structure is minimum over the region. The maximum response initially decreases with the increase in the values of electrical parameters and then again increases with them. The reason is for small values of the electrical parameters, the primary system has two peaks and then after certain values of the nondimensional parameters the system becomes unimodal and the peak response increases.

The optimal electrical parameters are found based on the minimum displacement of the primary mass. The values of $\alpha$ and $\kappa^2$ corresponding to the minimum value of the primary structure response provide a relationship between the two nondimensional parameters for the energy harvesting DVA. This gives the designer a wide range of values to select from. Note that values of nondimensional electrical parameters beyond these values will result in a single mode of vibration of the structure. Figure 7(*b*) shows the pairwise values of electrical parameters for which primary structure displacement attains the minimum. A fourth order polynomial curve (the dark line) is obtained numerically. It is to be noted that the position of this curve changes with the change in mass ratio $\mu$.

The relation in Fig. 7(*b*) is used to generate several pairs of nondimensional optimal electrical coefficients for which the primary structure has minimum displacement. These values therefore correspond to the most effective vibration control of the primary structure. These pairs of electrical coefficients are then used to generate curves for the frequency responses of the primary structure displacements (Fig. 8(*a*)) and for the power curves (Fig. 8(*b*)). For Figs. 8(*a*) and 8(*b*), the secondary structure damping is considered $\zeta_h = 0.1$. Note that in case of classical DVA the optimal value of damping $\zeta_h$ is 0.23 for mass ratio $\mu = 0.1$. As discussed before the single mode response curves is for the nondimensional time constant $\alpha = 0.50$, which is outside the curve in Fig. 7(*b*). The value of the nondimensional time constant for which the peak primary structure response is a minimum is 0.65. Figures 8(*a*) and 8(*b*) provide a tradeoff to choose the optimal nondimensional electrical parameters. Clearly $\alpha = 0.65$ shows a minimum value for the bimodal frequency response (as shown in Fig. 8), the best choice of nondimensional time constant $\alpha$ would

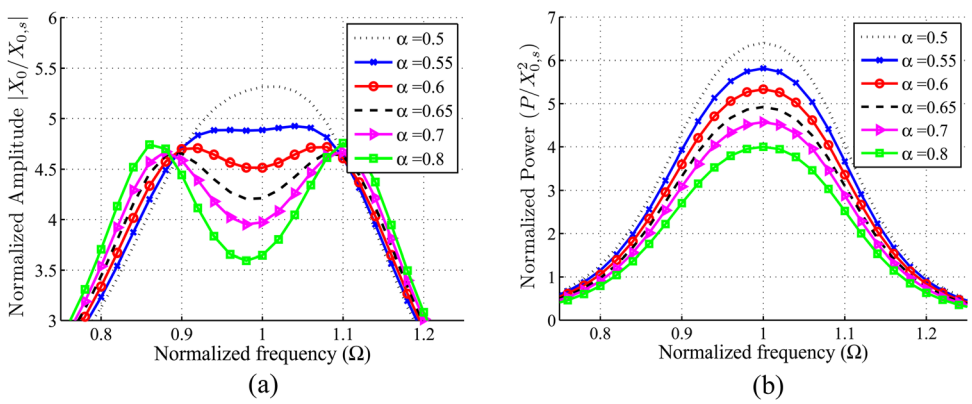


**Fig. 8 Frequency response curves of (*a*) normalized primary structure displacement and (*b*) normalized power (in mW/m$^2$) for mass ratio $\mu = 0.1$, damping $\zeta_h = 0.1$, and optimal frequency ratio. The nondimensional coupling coefficient $\kappa^2$ are chosen based on curve in Fig. 7(*b*) for nondimensional time constants given in the figures.**

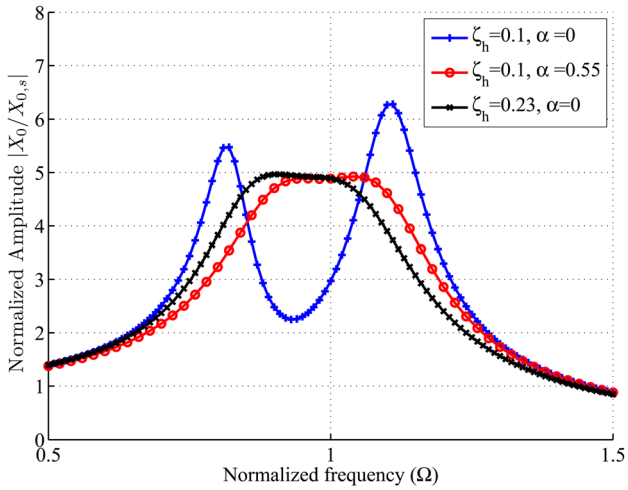


**Fig. 9 Frequency responses of primary structure displacement for classical DVA (i.e., with nondimensional time constant $\alpha = 0$ and nondimensional coupling coefficient $\kappa^2 = 0$) and energy harvesting DVA**

be 0.55. For a nondimensional time constant $\alpha = 0.55$ the amplitude of the frequency response of the primary structure displacement is almost the same as for $\alpha = 0.65$ but $\alpha = 0.55$ provides better power scavenging (see Fig. 8(*b*)). The curves in Fig. 8 are for normalized values and therefore true tradeoff is expected with actual variables and designer choice. In such a case the curve in Fig. 7(*b*) will become useful as it limits the choice of possible nondimensional electrical parameters.

A comparison of the classical DVA and the energy harvesting DVA is shown in Fig. 9. The frequency response curves for the primary structure displacement with nondimensional coupling coefficient $\kappa^2 = 0$. It is clear that for the same damping in the secondary structure $\zeta_h = 0.1$, energy harvesting DVA provides better control to that of classical DVA without energy harvesting capability. Classical DVA with optimal damping $\zeta_h = 0.23$ is also shown in Fig. 9. The frequency response curves for DVA with optimal damping and energy harvesting DVA with lesser damping have the same amplitude. This shows that the optimal damping requirement is reduced for a DVA if energy harvesting capability is added.

## 6 Conclusions

This article proposed the idea of a dynamic vibration absorber as an energy harvesting system. The aim is to reduce the vibration of a primary structure and simultaneously harvest energy from the vibration of an attached vibration absorber. A frequency domain method is proposed for the analysis and design of the coupled electromechanical system. A closed form expression for the optimal nondimensional frequency ratio of the decoupled system is derived. A detailed analysis of the damping of the EHDVA, nondimensional coupling coefficient, and nondimensional time constant are carried out. The main points arising from the present analysis are the following.

1. Unlike the classical DVA, energy harvesting DVA does not have any fixed points but it is shown that the fixed-point theory is approximately applicable for small values of electrical parameters.
2. A closed form explicit expression for the frequency ratio ($\beta$) is obtained as a function of the mass ratio $\mu$, nondimensional time constant $\alpha$, and nondimensional coupling coefficient $\kappa^2$. The expression can be further reduced to a function of $\mu$ and $\alpha$ with the help of some numerical analysis.
3. There exist a relation between the nondimensional electrical parameters that minimizes the primary structure vibrations. This relation changes with change in the mass ratio of the DVA.
4. The power scavenged by the harvester has a double peak frequency curve, which can used for broadband energy harvesting with a proper choice of parameters.
5. The addition of energy harvesting capacity of the DVA reduces the high damping requirement of the absorber for optimal performance.

Future work will include experimental demonstration of the proposed idea. Furthermore, the analytical work can be extended to active DVA (active tuned mass dampers) where the power required for the active control can be supplied by the harvested power.

## Acknowledgment

S.F.A. and S.A. acknowledge the support of the Royal Society through the award of the Newton International Fellowship and Wolfson Research Merit award, respectively.

## References

[1] Ali, S. F., and Ramaswamy, A., 2009, "Testing and Modeling of MR Damper and its Application to MDOF Systems Using Integral Backstepping Technique," ASME J. Dyn. Syst. Meas. Control, **131**(2), p. 021009.
[2] Sodano, H. A., Inman, D. J., and Park, G., 2004, "A Review of Power Harvesting From Vibration Using Piezoelectric Materials," Shock Vib. Dig., **36**(3), pp. 197–205.
[3] Priya, S., 2007, "Advances in Energy Harvesting Using Low Profile Piezoelectric Transducers," J. Electroceram., **19**(1), pp. 167–184.
[4] Beeby, S. P., Tudor, M. J., and White, N. M., 2006, "Energy Harvesting Vibration Sources for Microsystems Applications," Meas. Sci. Technol., **17**(12), pp. 175–195.
[5] Anton, S. R., and Sodano, H. A., 2007, "A Review of Power Harvesting Using Piezoelectric Materials (2003–2006)," Smart Mater. Struct., **16**(3), pp. R1–R21.
[6] Ali, S. F., Adhikari, S., Friswell, M. I., and Narayanan, S., 2011, "The Analysis of Piezomagnetoelastic Energy Harvesters Under Broadband Random Excitations," J. Appl. Phys., **109**(7), p. 074904.
[7] Lefeuvre, E., Badel, A., Benayad, A., Lebrun, L., Richard, C., and Guyomar, D., 2005, "A Comparison Between Several Approaches of Piezoelectric Energy Harvesting," J. Phys. IV, **128**, pp. 177–186.
[8] Lefeuvre, E., Badel, A., Richard, C., Petit, L., and Guyomar, D., 2006, "A Comparison Between Several Vibration-Powered Piezoelectric Generators for Standalone Systems," Sensors Actuators A Phys., **126**(2), pp. 405–416.
[9] Erturk, A., Hoffmann, J., and Inman, D. J., 2009, "A Piezomagnetoelastic Structure for Broadband Vibration Energy Harvesting," Appl. Phys. Lett., **94**(25), p. 254102.
[10] Litak, G., Friswell, M. I., and Adhikari, S., 2010, "Magnetopiezoelastic Energy Harvesting Driven by Random Excitations," Appl. Phys. Lett., **96**(21), p. 214103.
[11] Williams, C., and Yates, R., 1996, "Analysis of a Micro-Electric Generator for Microsystems," Sensors Actuators A Phys., **52**, pp. 8–11.
[12] Amirtharajah, R., and Chandrakasan, A., 1998, "Self-Powered Signal Processing Using Vibration-Based Power Generation," IEEE J. Solids State Circuits, **33**(5), pp. 687–695.
[13] Kulkarni, S., Koukharenko, E., Torah, R., Tudor, J., Beeby, S., O'Donnell, T., and Roy, S., 2008, "Design, Fabrication and Test of Integrated Micro-Scale Vibration-Based Electromagnetic Generator," Sensors Actuators A Phys., **145**, pp. 336–342.
[14] Sodano, H., Inman, D., and Park, G., 2005, "Comparison of Piezoelectric Energy Harvesting Devices for Recharging Batteries," J. Intel. Mater. Syst. Struct., **16**(10), pp. 799–807.
[15] Adhikari, S., Friswell, M. I., and Inman, D. J., 2009, "Piezoelectric Energy Harvesting From Broadband Random Vibrations," Smart Mater. Struct., **18**(11), p. 115005.
[16] Ali, S., Adhikari, S., and Friswell, M. I., 2010, "Piezoelectric Energy Harvesting With Parametric Uncertainty," Smart Mater. Struct., **19**(10), p. 105010.
[17] Sodano, H. A., Park, G., and Inman, D. J., 2004, "Estimation of Electric Charge Output for Piezoelectric Energy Harvesting," Strain, **40**(2), pp. 49–58.
[18] Stephen, N. G., 2006, "On Energy Harvesting From Ambient Vibration," J. Sound Vib., **293**, pp.409–425.
[19] Ng, T., and Liao, W., 2005, "Sensitivity Analysis and Energy Harvesting for a Self-Powered Piezoelectric Sensor," J. Intel. Mater. Syst. Struct., **16**(10), pp. 785–797.
[20] Cornwell, P., Goethals, J., Kowtko, J., and Damianakis, M., 2005, "Enhancing Power Harvesting Using a Tuned Auxiliary Structure," J. Intel. Mater. Syst. Struct., **16**, pp. 825–834.
[21] Beeby, S. P., Torah, R. N., Tudor, M. J., Glynne-Jones, P., O'Donnell, T., Saha, C. R., and Roy, S., 2007, "A Micro Electromagnetic Generator for Vibration Energy Harvesting," J. Micromech. Microeng., **17**(7), pp. 1257–1265.

[22] Nakano, K., Suda, Y., and Nakadai, S., 2003, "Self Powered Active Vibration Control Using a Single Electric Actuator," J. Sound Vib., **260**, pp. 213–235.
[23] Choi, Y. T., and Wereley, N. M., 2009, "Self Powered Magnetorheological Dampers," ASME J. Vib. Acoust., **131**, p. 044501.
[24] Chtiba, M. O., Choura, S., Nayfeh, A. H., and El-Borgi, S., 2010, "Vibration Confinement and Energy Harvesting in Flexible Structures Using Collocated Absorbers and Piezoelectric Devices," J. Sound Vib., **329**, pp. 261–276.
[25] Tang, X., and Zuo, L., 2010, "Regenerative Semi Active Control of Tall Building Vibration With Series TMDs," American Control Conference, Baltimore, MD, June 30–July 2, Vol. FrA12.1, pp. 5094–5099.
[26] Hartog, J. P. D., 1985, *Mechanical Vibrations*, Dover, New York.
[27] Caughey, T. K., and O'Kelly, M. E. J., 1965, "Classical Normal Modes in Damped Linear Dynamic Systems," ASME J. Appl. Mech., **32**, pp. 583–588.
[28] Adhikari, S., 2006, "Damping Modelling Using Generalized Proportional Damping," J. Sound Vib., **293**(1–2), pp. 156–170.
[29] Ormondroyd, J., and Hartog, J. P. D., 1928, "Theory of the Dynamic Vibration Absorber," Trans. Am. Soc. Mech. Eng., **50**, pp. 9–22.
[30] Randall, S. E., Halsted, D. M., and L. Taylor, D., 1981, "Optimum Vibration Absorber for Linear Damped System," ASME J. Mech. Design, **103**, pp. 908–913.
[31] Zhu, S. J., Zheng, Y. F., and Fu, Y. M., 2004, "Analysis of Non-Linear Dynamics of a Two-Degree-of-Freedom Vibration System With Non-Linear Damping and Non-Linear Spring," J. Sound Vib., **271**(1–2), pp. 15–24.
[32] Liu, K., and Coppola, G., 2010, "Optimal Design of Damper Dynamic Vibration Absorber for Damped Primary Systems," Trans. Can. Soc. Mech. Eng., **34**(1), pp. 119–135.
[33] Thompson, A. G., 1980, "Optimizing the Untuned Viscous Dynamic Vibration Absorber With Primary System Damping: A Frequency Locus Method," J. Sound Vib., **77**, pp. 469–472.
[34] Pennestri, E., 1998, "An Application of Chebyshev's Min-Max Criterion to the Optimum Design of a Damped Dynamic Vibration Absorber," J. Sound Vib., **217**, pp. 757–765.
[35] Brown, B., and Singh, T., 2011, "Minimax Design of Vibration Absorbers for Linear Damper Systems," J. Sound Vib., **330**, pp. 2437–2448.
[36] Ghosh, A., and Basu, B., 2007, "A Closed-Form Optimal Tuning Criterion for TMD in Damped Structures," Struct. Control Health Monitor., **14**, pp. 681–692.
[37] Dutoit, N. E., Wardle, B. L., and Kim, S.-G., 2005, "Design Consideration For MEMS Scale Piezoelectric Mechanical Vibration Energy Harvesters," Integrated Ferroelectrics Int. J., **71**(1), pp. 121–160.